Primljen / Received: 30.9.2024.
Ispravljen / Corrected: 23.8.2025.
Prihvaćen / Accepted: 1.9.2025.
Dostupno online / Available online: 10.1.2026.

Orthogonal test-based study on mechanical properties of coal-fired slag concrete

Authors:

Jianpeng Zhang, MCE
Yili Normal University, China
College of Physical Science and Technology
17041@ylnu.edu.cn

Prof. **Gang Li**, PhD. CE
Shihezi University, China
College of Water Conservancy and Architecture
gangli@shzu.edu.cn
Corresponding author

Jiamin Liu, MCE
Xinjiang Academy of Agricultural and Reclamation Sciences, China
Logistics Service Centre
liujiamin1205@163.com

Ling Li, MCE
Zhongming Engineering Design Consulting Co., China
m15099196374 @163.com

Research Paper

Jianpeng Zhang, Gang Li, Jiamin Liu, Ling Li

Orthogonal test-based study on mechanical properties of coal-fired slag concrete

To improve the incorporation of coal-fired slag into concrete, this study investigated the effects of several key factors on the mechanical properties of coal-fired slag concrete using orthogonal testing. The parameters studied included water-binder ratio (0.45, 0.475, 0.5, and 0.525), fly ash replacement ratio (0, 10, 20, and 30 %), sand ratio (37.5, 40, 42.5, and 45 %), and coal-fired slag replacement ratio (0, 33.33, 66.67, and 100 %). The effects of these factors on the seventh, 14th, and 28th-day compressive strengths, as well as the 28th day splitting tensile strength, were examined. A microscopic analysis was performed via SEM to explore the surface characteristics of the concrete. The results revealed a gradual decrease in concrete strength as the water-binder ratio and coal-fired slag replacement ratio increased. The water-binder ratio significantly affected both the compressive and splitting tensile strengths. The optimal concrete mix, consisting of a water-binder ratio of 0.45, fly ash replacement ratio of 10%, sand ratio of 45%, and coal-fired slag replacement ratio of 66.67 %, resulted in a 28-day compressive strength of 42.18 MPa and splitting tensile strength of 3.21 MPa. These values satisfy the C30 strength requirements for structural building applications, enhancing the economic value of coal-fired slag and broadening the potential uses of slag concrete.

Key words:
orthogonal test, coal-fired slag concrete, compressive strength, splitting tensile performance, microstructure

Prethodno priopćenje

Jianpeng Zhang, Gang Li, Jiamin Liu, Ling Li

Ispitivanje mehaničkih svojstava betona sa zgurom iz ugljena pomoću ortogonalnoga eksperimentalnog plana

Kako bi se poboljšala ugradnja zgure iz ugljena u beton, u ovom su istraživanju ortogonalnim eksperimentalnim planom ispitani učinci nekoliko ključnih čimbenika na mehanička svojstva betona sa zgurama od izgaranja ugljena. Proučavani parametri uključivali su vodocementni omjer (0,45, 0,475, 0,5 i 0,525), omjer zamjene letećim pepelom (0, 10, 20 i 30 %), omjer pijeska (37,5, 40, 42,5 i 45 %) i omjer zamjene zgurom iz ugljena (0, 33,33, 66,67 i 100 %). Ispitani su učinci tih čimbenika na tlačnu čvrstoću nakon 7, 14 i 28 dana te na vlačnu čvrstoću cijepanjem nakon 28 dana. Mikroskopska analiza provedena je pomoću SEM-a kako bi se istražile karakteristike površine betona. Rezultati su pokazali postupno smanjenje čvrstoće betona s povećanjem omjera vode i veziva te omjera zamjene zgurom iz ugljena. Omjer vode i veziva znatno je utjecao i na tlačnu i vlačnu čvrstoću. Mješavina betona s najboljim svojstvima, koja se sastoji od omjera vode i veziva od 0,45, omjera zamjene letećim pepelom od 10 %, omjera pijeska od 45 % i omjera zamjene zgurom iz ugljena od 66,67 %, rezultirala je tlačnom čvrstoćom od 42,18 MPa nakon 28 dana i vlačnom čvrstoćom od 3,21 MPa. Vrijednosti su u skladu sa zahtjevima razreda čvrstoće C30 za nosive građevinske konstrukcije, što pridonosi većoj gospodarskoj vrijednosti zgure od izgaranja ugljena i širi mogućnosti primjene betona sa zgurom.

Ključne riječi:
ortogonalni eksperimentalni plan, beton sa zgurom iz ugljena, tlačna čvrstoća, vlačna čvrstoća, mikrostruktura

1. Introduction

According to the China Energy Development Report 2023, China's raw coal production significantly increased, reaching 4.56 billion tonnes by 2022, which is a 10.5 % increase compared to the previous year [1, 2]. Additionally, by 2022, thermal power generation reached 5,077 billion kilowatt-hours, accounting for nearly 70 % of China's total power output. This highlights the continued dominance of thermal power in the nation's electricity sector [3, 4].

Coal combustion generates significant amounts of slag, which poses environmental challenges. However, only a small fraction of this slag is recycled for applications, such as road filling and brick manufacturing [5-7]. Most slag is either left in open-air piles or discarded in landfills, leading to considerable degradation of air and soil quality in the surrounding environment [8, 9].

With increasing environmental concerns, the resourceful use of industrial solid waste, including coal-fired slag, has become a prominent research topic. Stijanović and Memiș explored the incorporation of industrial waste in building materials [10, 11]. Numerous studies have explored effective management strategies and applications for this material [12-15]. Itaru et al. [16] investigated the feasibility of using coal gasification slag as a fine aggregate replacement in concrete. They found that when the slag substitution rate was maintained at or below 25 %, the strength characteristics of the concrete either remained the same or improved compared with those of conventional concrete. Zhang et al. [17] achieved 80 % replacement of traditional materials with coal-fired slag to produce C20 road concrete. Geçkil et al. [18] studied the preparation of road concrete using blast furnace slag. The results indicated that concrete containing 20 % blast furnace slag exhibited superior performance. Murko et al. [19] investigated the composition of ash from coal-fired power plants and explored the potential use of this ash as a raw material for cement production. Guo et al. [20] examined the application of coal-fired slag in subterranean engineering, focusing on the correlation between the fractal dimension of concrete and its compressive strength using scanning electron microscopy. Their findings revealed a gradual decrease in the compressive strength as the proportion of coal-fired slag increased. Sandip et al. [21] explored the use of coal-fired bottom ash and slag as a partial cement replacement. Their study showed that concrete incorporating 10 % coal-fired bottom ash exhibited enhanced tensile strength, elastic modulus, and durability. Similarly, Zhang et al. [22] developed self-compacting concrete using coal-fired slag as an aggregate. This concrete exhibited an apparent density of 1645.5 kg/m^3 and a compressive strength of 16.3 MPa, making it suitable for non-structural components in construction. Liu et al. [23-25] developed concrete with a high coal-fired slag replacement ratio of 85.8 %. This formulation achieved a compressive strength of 15 MPa, making it suitable for applications such as flooring in the Yangchangwan coal mines. Despite the significant advancements in the use of coal slag in concrete, the low strength of coal slag concrete remains a challenge. Consequently, its applications are primarily limited to specific areas, such as roads and indoor partitions, particularly non-structural components [17, 18, 22, 25]. This significantly restricts the application of coal-fired slag in construction.

In summary, concrete with a high slag content often exhibits low strength, which limits its engineering applications. To ensure that slag concrete meets the strength requirements of construction projects, the amount of slag used is typically reduced, leading to a lower slag utilisation. Therefore, it is essential to identify the optimal amount of slag admixture that significantly enhances its utilisation rate while ensuring that the strength of concrete is suitable for widespread application.

The main objective of this study was to address the challenge of low-strength coal-fired slag concrete by investigating the use of a significant proportion of coal-fired slag in the production of structural engineering-grade C30 concrete. Using an orthogonal design experimental approach, various factors such as the water-cement, fly ash replacement, sand, and coal-fired slag replacement ratios were investigated. This study aimed to explore the impact of these factors on the mechanical properties of coal-fired slag concrete through comprehensive experimentation. The goal was to identify the optimal composition of coal-fired slag concrete, offering valuable insights and guidelines for improving its application in construction projects and enhancing its viability and effectiveness in structural engineering.

2. Materials and methods

2.1. Materials

Portland cement (P-O, 42.5) supplied by the Xinjiang Shihezi Nanshan Cement Plant was used in this study. The physical, mechanical, and chemical properties of the cement, as detailed in Table 1, conformed to Chinese national standard GB175-2007 [26]. Fly ash (FA) was sourced from Xinjiang Yue Long Da Renewable Resources Technology Co. The FA parameters are listed in Table 2. The particle size distribution of the FA is presented in Figure 1.

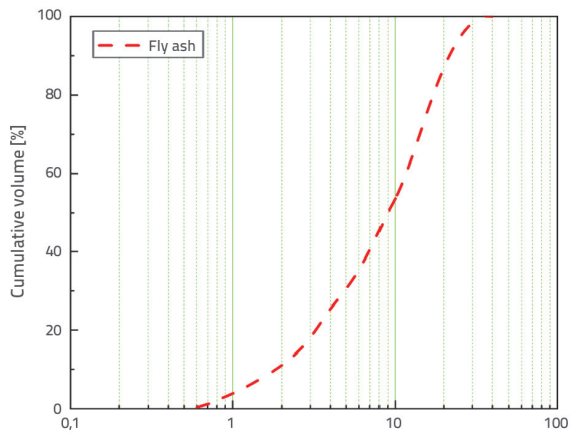

Figure 1. Particle size distribution curves of fly ash

Table 1. Properties of the cement used in the study

Properties	Cement	Limit as per GB175-2007
Specific surface area [m²/kg]	356.4	Minimum 300
Soundness: pat test	Pass	No cracks or bends
Initial setting time [min]	178	Minimum 45
Final setting time [min]	228	Maximum 600
Third-day compressive strength [MPa]	30.6	Minimum 22.0
Third-day flexural strength [MPa]	6.4	Minimum 4.0
MgO [%]	2.13	Maximum 5.0
SO_3 [%]	2.58	Maximum 3.5
LOI [%]	1.10	Maximum 5.0

Table 2. Parameters of fly ash

Grade	Fineness [%]	Loss on ignition [%]	Water demand ratio [%]	Moisture content [%]
I	7.7	2.1	94	0.3

Medium sand with a fineness modulus of 2.84 was used as the fine aggregate. Pebbles with a maximum particle size of 20 mm were used as the coarse aggregates. HSC polycarboxylic acid was used as a water-reducing agent at a water-reducing ratio of 15 wt %. Municipal tap water was used for all tests.

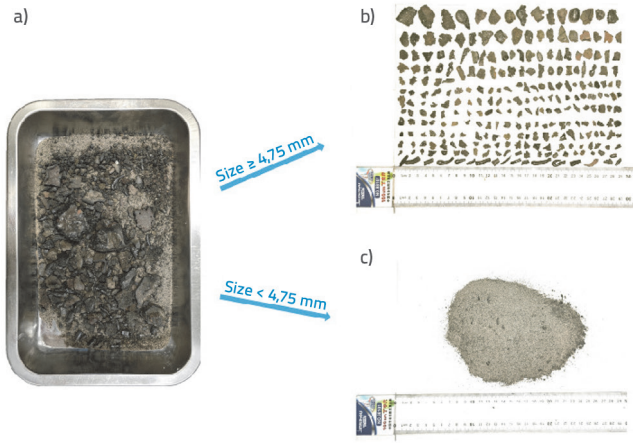

Figure 2. Power-plant coal furnace slag

Power plant coal-fired slag appears in various forms, including large and small blocks, powders, and particles of different sizes, as shown in Figure 2.a. These often contain millimetre- and micron-level holes, resulting in a loose structure that is unsuitable for direct use in concrete. Therefore, preliminary crushing and screening are required to prepare the coal slag for incorporation into concrete. Particles larger than 4.75 mm, owing to their porous and lightweight nature, are suitable as complete or partial replacements for coarse aggregates in concrete, as shown in Figure 2.b. This substitution enhances the permeability, thermal insulation, and lightweight properties of concrete. In contrast, coal-fired slag particles smaller than 4.75 mm can replace fine aggregates in standard concrete mixtures, as shown in Figure 2.c.

For this study, preliminary crushed slag was sourced from the Shihezi South Thermal Power Plant. The selected slag particles were smaller than 5 mm, with a fineness modulus of 2.34, bulk density of 834 kg/m³, and moisture content of 5.4 %. The chemical compositions of the slags are listed in Table 3. The particle size distributions of the coal-fired slag and sand are shown in Figure 3.

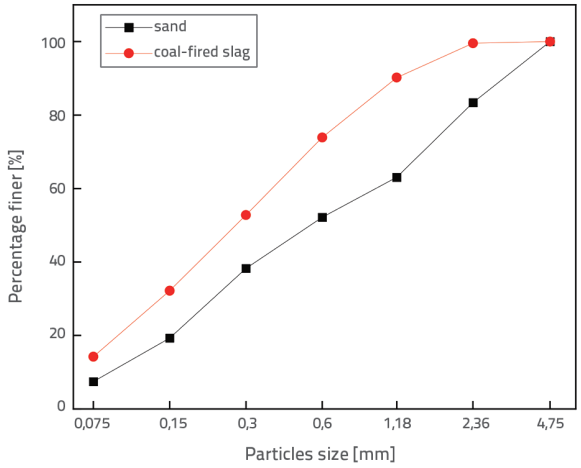

Figure 3. Particle size distribution curves of sand- and coal-fired slags

Table 3. Chemical composition of coal-fired slag [%]

SiO_2	Al_2O_3	CaO	Fe_2O_3	TiO_2	SO_3	MgO	K_2O	Na_2O	LOI
42.16	16.85	12.64	10.12	0.86	9.96	3.78	1.15	1.92	0.56

Table 4. Experimental factor levels

Level	Water-cement ratio A	Fly ash replacement ratio B	Sand ratio C	Coal-fired slag replacement ratio D	Empty column E
1.	0.45	0	37.5 %	0	1
2.	0.475	10 %	40 %	33.33 %	2
3.	0.5	20 %	42.5 %	66.67 %	3
4.	0.525	30 %	45 %	100 %	4

Table 5. Concrete material mix ratio

Broj	Considerations					Water [kg/m³]	Cement [kg/m³]	Fly ash [kg/m³]	Slags [kg/m³]	Sand [kg/m³]	Rock [kg/m³]	Water-reducing agente vod [kg/m³]
	A	B	C	D	E							
1#	1	1	1	1	1	175	389	0	0	700	1166	7
2#	1	2	2	2	2	175	350	39	249	498	1120	7
3#	1	3	3	3	3	175	311	78	528	265	1073	7
4#	1	4	4	4	4	175	272	117	840	0	1026	7
5#	2	1	2	3	4	175	368	0	503	252	1132	7
6#	2	2	1	4	3	175	332	37	707	0	1179	7
7#	2	3	4	1	2	175	295	74	0	849	1038	7
8#	2	4	3	2	1	175	258	111	267	535	1085	7
9#	3	1	3	4	2	175	350	0	810	0	1095	6
10#	3	2	4	3	1	175	315	35	571	286	1048	6
11#	3	3	1	2	4	175	280	70	238	476	1191	6
12#	3	4	2	1	3	175	245	105	0	762	1143	6
13#	4	1	4	2	3	175	333	0	288	577	1057	6
14#	4	2	3	1	4	175	300	33	0	817	1105	6
15#	4	3	2	4	1	175	267	67	769	0	1153	6
16#	4	4	1	3	2	175	233	100	480	241	1201	6

2.2. Orthogonal experimental designs

In this study, the mix proportion design for coal-fired slag concrete adhered to the guidelines specified in JGJ 55-2011 "Specification for mix proportion design of ordinary concrete" [27]. The compressive and splitting tensile strengths of concrete were selected as the evaluation criteria for experimental results. An orthogonal experimental approach was employed to investigate the effects of four key factors, namely the water-cement ratio (Factor A), fly ash replacement rate (Factor B), sand ratio (Factor C), and coal-fired slag replacement rate (Factor D). The range of variation for Factor A was established through a one-way test as 0.45 to 0.525. Factor B ranged from 0 % to 30 %; Factor C varied from 37.5 % to 45 %; and Factor D, the primary focus of the orthogonal test, ranged from 0 % to 100 %. The experiments were organised using the orthogonal table L16 (4^5), with one blank column used as the control (Column E). Four different levels were established for each factor, as listed in Table 4. The ratios listed in Table 4 are expressed in mass proportions.

In this experiment, the levels of coal-fired slag replacement were defined as follows: Level 1 represented 0 % slag replacement, where only sand was used as the fine aggregate, and Level 4 corresponded to 100 % coal-fired slag replacement, with coal-fired slag exclusively used as the fine aggregate.

For this test, 16 sets of material ratios were determined, corresponding to the specific levels of each key factor outlined in Table 5. These ratios were systematically calculated by analysing and combining the various water–cement, fly ash replacement, sand, and coal slag replacement ratios used in the experiment.

2.3. Specimen production and test methods

The concrete preparation process is depicted in Figure 4. After mixing, the concrete was poured into moulds to create 100 × 100 × 100 mm test blocks. After curing for one day, the moulds were removed, and the concrete blocks were transferred to a standard curing room maintained at a temperature of 20±1°C and relative humidity of 90 %±5 % for 28 days of further curing.

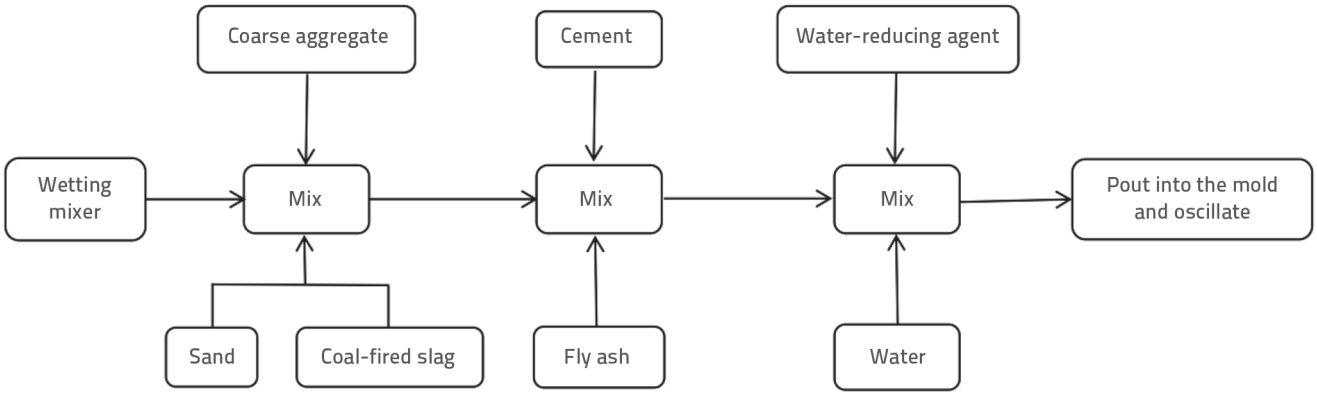

Figure 4. Sample preparation

Table 6. Mechanical and workability test results for slag concrete

Number	Compressive strengths [MPa]			28-day splitting tensile strength [MPa]	Slump [mm]
	7 days	14 days	28 days		
1#	35.40	38.58	45.39	3.35	256
2#	33.41	36.88	43.50	3.29	238
3#	30.48	33.16	41.28	3.17	155
4#	28.72	31.62	40.15	3.11	52
5#	29.19	33.61	39.96	3.00	187
6#	28.63	31.74	37.14	2.91	22
7#	32.59	36.52	41.12	3.08	197
8#	30.52	34.82	39.71	2.98	216
9#	28.08	30.36	35.92	2.70	23
10#	28.03	31.08	36.93	2.76	146
11#	29.20	31.73	39.02	3.00	223
12#	30.58	32.21	38.20	3.08	184
13#	26.86	30.11	35.28	2.74	207
14#	28.59	31.97	37.24	2.81	219
15#	25.87	28.11	32.90	2.30	18
16#	26.44	29.01	34.03	2.36	120

Following the GB/T 50080-2016 "Standard for Test Methods of Properties of Ordinary Concrete Mixes" [28], the workability of the freshly mixed concrete was evaluated. The compressive strength of the concrete was measured after 7, 14, and 28 days, while the tensile splitting strength was assessed at 28 days, according to GB/T 50081-2019 "Standard for Test Methods of Physical and Mechanical Properties of Concrete" [29]. Three cubic specimens with dimensions of 100 × 100 × 100 mm were prepared for each test to measure the compressive strength and splitting tensile strength of concrete. The arithmetic mean of the test values of the three specimens was considered the strength value of the final specimen. If the difference between the maximum or minimum test value and median value exceeded 15 % of the median value, the maximum and minimum test values were excluded, and the median value was used as the test result. Because of the use of nonstandard specimens for testing, the compressive strength and split tensile strength of the cube were multiplied by corresponding size-conversion factors. The dimensional conversion factors were 0.95 for the cubic compressive strength and 0.85 for split tensile strength.

Scanning electron microscopy (SEM; ZEISS Gemini, Germany) was used to study micro-interfaces. SEM facilitated the detailed analysis and characterisation of concrete sample interfaces, offering valuable insights into their microstructural properties. Additionally, the hydration reaction of slag concrete was investigated using an X-ray diffractometer (D8 ADVANCE; Bruker AXS, Germany) to examine the physical phases of the hydration products at seven and 28 days. This advanced instrument enabled the comprehensive characterisation of the hydration products, providing insights into the chemical processes within slag concrete.

Table 6 summarises the results of various tests performed on freshly mixed concrete cubes, including the compressive strengths at seven, 14, and 28 days, split tensile strength at 28 days, and slump. These results provide valuable insights into the mechanical properties of concrete samples.

3. Results analysis

3.1. Working performance analysis

The slump test results presented in Table 6 show significant variations in the workability of coal-fired slag concrete across different groups. In particular, the groups with 0 % and 33.33 % coal-fired slag replacement ratios (1#, 2#, 7#, 8#, 11#, 12#, 13#, and 14#) exhibited slumps exceeding 180 mm, thereby demonstrating favourable workability. In contrast, groups with a 66.67 % coal-fired slag replacement ratio (3#, 5#, 10#, and 16#) had slumps ranging from 120 mm to 180 mm, indicating normal workability. Notably, groups with a 100 % coal-fired slag replacement ratio (4#, 6#, 9#, and 15#) had slumps of less than 60 mm, indicating significantly poor workability.

Specifically, in Groups 4#, 6#, 9#, and 15#, where coal-fired slag concrete was used at a 100 % coal-fired slag replacement ratio, the mixtures exhibited loose textures with poor bonding between the aggregates. During loading into test moulds and vibration, water segregation occurred, indicating weak cohesion. This observation can be attributed to the high water-absorption capacity and presence of micropores in the coal-fired slag particles, which absorb significant amounts of water and act as a water-reducing agent. Consequently, insufficient amounts of water and water-reducing agents were absorbed by cementitious materials, resulting in extremely poor concrete cohesion. During initial curing stages, the water absorbed within the coal-fired slag particles is released into the environment, leading to poor water retention. These findings are consistent with the trial results reported by Malkit et al. [30].

Based on the observed performance of coal-fired slag concrete, special attention must be paid to the moulding process when preparing concrete with 100 % slag replacement.

3.2. Intensity extreme variance analysis

An extreme variance analysis was used to assess the sensitivity of the factors to the impacts of the indicators. The sensitivities of the factors were determined by calculating the magnitude of the extreme difference, R. The size of R reflects the changes in the test indicators resulting from fluctuations in the levels of the factors, with a larger R indicating a more significant impact of the factor on the test indicators. SPSS software was used to analyse the mechanical property test results, as shown in Table 6. The R-values for extreme differences were calculated to evaluate the influence of each factor on the experimental outcomes. Table 7 summarises the results of extreme difference analysis. A extreme difference analysis indicated that each factor affected the compressive and split tensile strengths of slag concrete differently at various curing stages.

At seven days, the compressive strength of coal-fired slag concrete was primarily influenced by the water-cement ratio (A), followed by the coal-fired slag replacement ratio (D), sand ratio (C), and fly ash replacement ratio (B). By the 14th day, the water-cement ratio (A) remained the most significant factor affecting the compressive strength, followed by the coal-fired slag replacement ratio (D), fly ash replacement ratio (B), and sand ratio (C). At 28 days, both the compressive and split tensile strengths were most influenced by the water-cement ratio (A), followed by the coal-fired slag replacement ratio (D), fly ash replacement ratio (B), and sand ratio (C).

These results highlight the importance of managing the water-cement ratio and optimising the coal-fired slag replacement ratio to enhance the strength characteristics of slag concrete across different curing periods. Adjusting the fly ash replacement and sand ratios can also contribute to achieving the desired performance of slag concrete formulations.

3.3. Determination of the optimal ratio

Several analyses were performed to illustrate the impact of different factor levels on the mechanical properties of coal-fired slag concrete. The plots depict the relationship between the factor levels (horizontal axis) and seven, 14, and 28-day compressive strengths, as well as the 28-day splitting tensile strength (vertical axis). Figures 5–8 show these relationships and provide a visual interpretation of the data.

Table 7. Extreme variance analysis of the mechanical properties of slag concrete

Number	7-day compressive strength [MPa]				14-day compressive strength [MPa]				28-day compressive strength [MPa]				28-day splitting tensile strength [MPa]			
	A	B	C	D	A	B	C	D	A	B	C	D	A	B	C	D
k1j	32.00	29.88	29.92	31.79	35.06	33.16	32.76	34.82	42.58	39.14	38.90	40.49	3.23	2.94	2.91	3.08
k2j	30.23	29.66	29.76	30.00	34.17	32.91	32.70	33.39	39.48	38.70	38.64	39.38	2.99	2.94	2.92	3.00
k3j	28.97	29.54	29.42	28.54	31.35	32.38	32.58	31.71	37.52	38.58	38.54	38.05	2.88	2.89	2.91	2.82
k4j	26.94	29.06	29.05	27.82	29.80	31.92	32.33	30.46	34.86	38.02	38.37	36.53	2.55	2.88	2.92	2.76
R	5.06	0.82	0.87	3.97	5.26	1.25	0.43	4.36	7.72	1.11	0.53	3.96	0.68	0.06	0.02	0.32

Note: k1j represents the mean of the results of the tests in column j related to factor level 1; and R is the extreme variance.

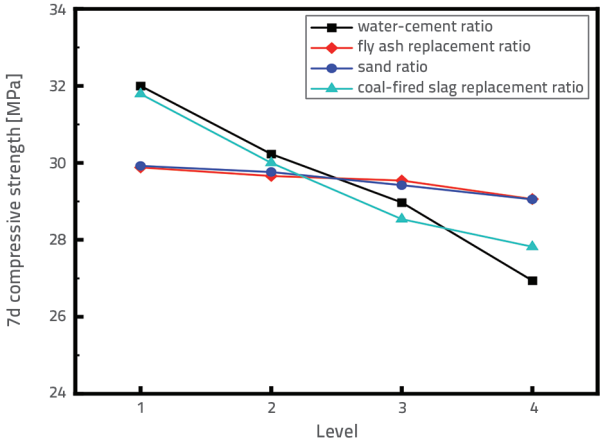

Figure 5. Effect of different factors on the seven-day compressive strength of coal-fired slag concrete

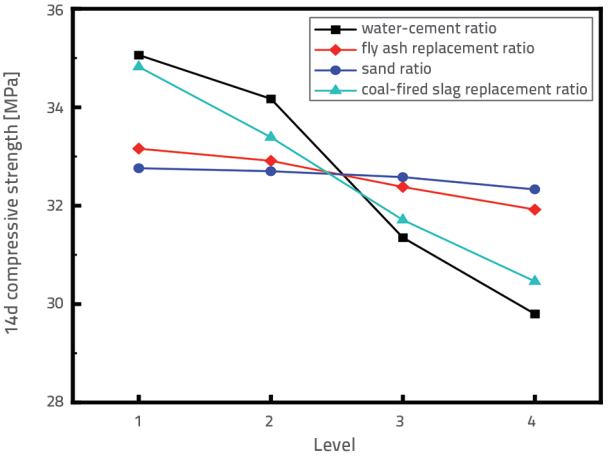

Figure 6. Effect of different factors on the 14-day compressive strength of coal-fired slag concrete

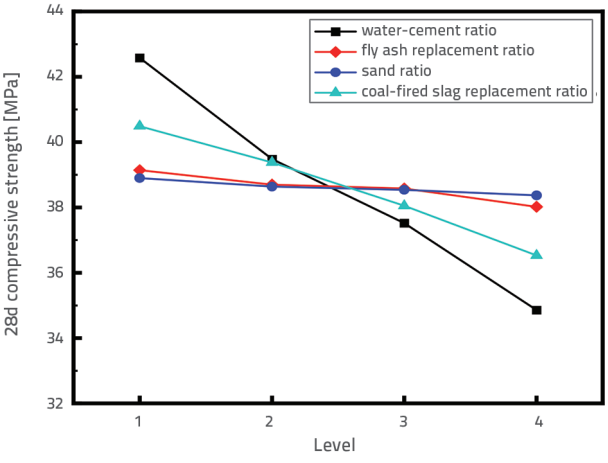

Figure 7. Effect of different factors on the 28-day compressive strength of coal-fired slag concrete

Based on the data in Table 6 and trends observed in Figures 5–8, the compressive strengths at seven, 14, and 28 days, as well as the 28-day splitting tensile strength, of the coal-fired slag concrete decreased with increasing water–cement ratio and coal-fired slag replacement ratio. The effects of the sand and fly ash replacement ratios on concrete strength were relatively weak.

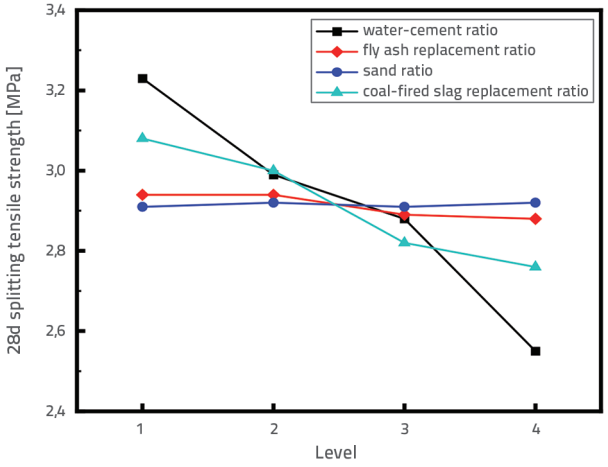

Figure 8. Effect of different factors on the 28-day splitting tensile strength of coal-fired slag concrete

The study employed a relatively high water–cement ratio owing to the high water-absorption rate of coal-fired slag. When incorporated into a concrete mix, the coal-fired slag absorbs water without consuming it. During the curing process, this absorbed water is lost, creating pore spaces within the concrete. This reduction in compactness decreased the strength of the coal-fired slag concrete as the water-cement ratio increased.

The loose structure of the coal-fired slag particles compromised the overall structural integrity of the concrete. As the coal-fired slag replacement ratio increased, these structural weaknesses became more pronounced, leading to a gradual decrease in strength. A higher replacement ratio exacerbates these deficiencies. Incorporating nanofibres can address these issues by improving matrix densification, thereby enhancing both the durability and sustainability of concrete.

As the coal-fired slag replacement ratio increases, both the working performance and compactness of the concrete deteriorate. As shown in Figure 9, at a 100 % replacement ratio, numerous voids appeared on the sidewalls of the moulded specimens. These internal defects further compromised the strength of the concrete.

The fly ash replacement ratio mainly influences the mechanical properties of the coal-fired slag concrete at the later stages of strength development. Although its effect on the seven-day compressive strength was relatively minor, it became more significant on days 14 and 28. This is likely owing to the pozzolanic reaction of fly ash, where its particles interact with calcium hydroxide in concrete to form hydrated calcium silicate and aluminate, thereby enhancing the strength over time [31]. These reaction products fill the voids between the concrete aggregates, enhancing the densification of the concrete

structure and improving its strength in later stages. As shown in Figures 5–8, the strength of slag concrete remained relatively stable with fly ash dosages of 10 % or less. However, when the dosage exceeded 10 %, the strength of the concrete decreased. This reduction in strength occurred because, at higher dosages, only a small portion of the fly ash participated in the hydration reaction. The remaining fly ash did not contribute to the reaction, which diminished the overall activity of the cement paste and led to a decrease in strength [32].

Finally, the sand ratio had the least impact on the concrete strength, though it still contributed to a reduction. As the sand ratio increased, the total surface area of the concrete aggregates also increased. The fixed amount of cementitious material led to reduced bonding between the aggregates, thereby decreasing the concrete strength. However, the effect was limited; in the tested range, increasing the sand ratio from 37.5 % to 45 % resulted in a 1.4 % reduction in compressive strength.

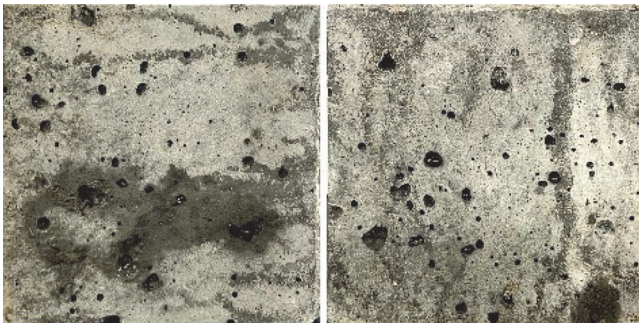

Figure 9. Typical concrete sidewall with 100 % slag replacement

An analysis of Figures 5–8 demonstrated that Level 1 of the selected factors performed the best across various test indicators. However, at this level, both the fly ash and coal-fired slag replacement ratios were 0 %, which does not align with the goal of utilising industrial solid waste. Therefore, a more comprehensive analysis of the test results is necessary.

For the water-cement ratio, a level of 0.45 demonstrated the optimal effect on the test indicators. Regarding the fly ash replacement ratio, Level 1 was excluded. In Figure 7, Levels 2 and 3 have negligible impacts on the compressive strength, and in Figure 8, Level 2 outperforms Level 3 in splitting tensile strength. Therefore, Level 2 is more appropriate for fly ash replacement.

The sand ratio had a negligible effect on the test results. However, Level 4, which allowed for a higher proportion of fine aggregates, was more suitable because it supported a higher coal-fired slag ratio.

Based on the previous discussion, although level 4 was initially deemed appropriate as the coal-fired slag replacement ratio, it exhibited poor workability. Excluding Levels 1 and 4, the analysis of Figure 7 reveals that at Level 2, the compressive strength is 39.38 MPa, while at Level 3, it is 38.05 MPa, showing only a 3.4 % reduction in strength. Given the significant increase in the coal-fired slag replacement ratio from Level 2 to Level 3, Level 3 is deemed more reasonable for enhancing slag utilisation.

In summary, the optimal proportions for coal-fired slag concrete are as follows: a water-cement ratio of 0.45, fly ash replacement rate of 10 %, sand ratio of 45 %, and coal-fired slag replacement ratio of 66.67 %. At this optimal proportioning scheme, the freshly mixed coal-fired slag concrete achieved a slump of 187 mm, 28-day compressive strength of 42.18 MPa, and splitting tensile strength of 3.21 MPa. These values meet the requirement that the concrete strength grade for reinforced concrete structural members should not be lower than C25, as specified in GB55008-2021 "General Specification for Concrete Structures" [33]. Compared to standard concrete, the new mix design decreases the use of river sand by approximately 66.67 %, thereby reducing its impact on river ecosystems. Additionally, this substantially increases the incorporation of slag, thereby enhancing the economic benefits of using slag. However, this mixed design results in a strength reduction of approximately 7.1 %.

3.4. Calculation formula for compressive and splitting tensile strengths

Using the mechanical property test results from Table 6, a regression analysis was conducted to explore the relationship between the 28-day compressive and split tensile strengths of coal-fired slag concrete. This analysis yielded an empirical formula that captured the correlation between the two key strength parameters. A fitting curve illustrating this relationship is shown in Figure 10.

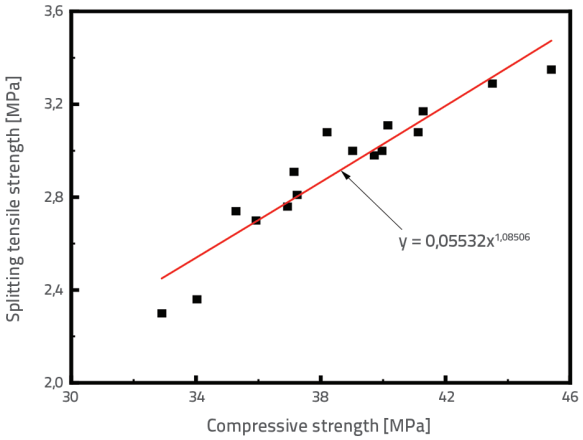

Figure 10. Relationship between compressive strength and splitting tensile strength

3.5. SEM analysis

To gain deeper insights into the strength variation mechanisms in coal-fired slag concrete, the microscopic structure of each component was examined via SEM. Samples from concrete groups 1#, 9#, and 11# were selected for the analysis. Group 1# used river sand as the fine aggregate, Group 9# used coal-fired slag as the fine aggregate, and Group 11# incorporated a mixture of river sand (66.67 %) and coal-fired slag (33.33 %).

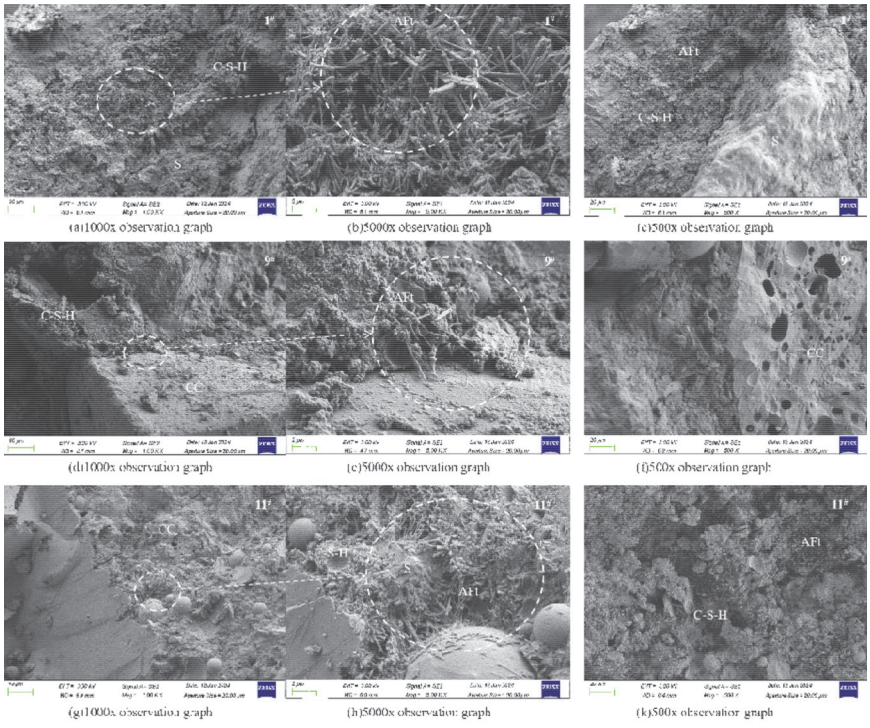

Figure 11. SEM image of coal-fired slag concrete-based phase interface (samples 1#, 9#, and 11#)

SEM observations were conducted to examine the micro-morphologies of the three groups of specimens, with a particular focus on the base-phase interface of the coal-fired slag concrete. Figure 11 presents the SEM images of the micro-interfaces of samples from concrete groups 1#, 9#, and 11# after 28 days of curing.

The SEM analysis of sample 1# (Figures 11.a and 11.b) shows dense formations of needle- and rod-shaped calcite (AFt) and clusters of hydrated calcium silicate (C-S-H) around the aggregate. These minerals fill the gaps between aggregates, thereby enhancing the density and strength of concrete structures. In sample 9# (Figures 11.d and 11.e), calcite was also present around the coal-fired slag particles but in smaller amounts compared with that in sample 1#, resulting in weaker connections and reduced cement hydration. For sample 11# (Figures 11.g and 11.h), significant amounts of calcite and hydrated calcium silicate were present around the aggregate. The interface of the ruptured coal-fired slag (CC) showed unevenly distributed micropores. The degree of cement hydration in sample 11# was intermediate between those of samples 1# and 9#.

At 500 × magnification (Figures 11.c, 11.f and 11.k), SEM scans of samples 1# and 11# displayed well-hydrated products among the three sample groups. In contrast, sample 9# showed noticeable micropores at the interface of the damaged coal-fired slag particles. Additionally, the aggregates in sample 9# appeared more intact than those in sample 1#, indicating that failure in the coal-fired slag concrete primarily occurred through the fracture and damage of the coal-fired slag particles. During the concrete curing process, the moisture released from coal-fired slag particles triggered a hydration reaction with the cementitious materials on their surfaces. This reaction led to the formation of ettringite and hydrated calcium silicate on the surface of the coal-fired slag particles, thereby enhancing their strength compared to the original untreated coal-fired slag particles [34]. However, under ultimate load conditions, the coal-fired slag particles were the first to fracture and cause damage, leading to the overall failure of the concrete.

A microscopic analysis revealed that the strength of the coal-fired slag concrete was closely related to the extent of hydration and quantity of slag used. A higher degree of hydration resulted in a denser concrete matrix with fewer voids, thereby enhancing the strength of the concrete. Conversely, a lower slag content reduced the presence of weak zones within the concrete structure, leading to higher strength. This observation is consistent with the mechanical properties of concrete. For instance, sample 1, which exhibited the most complete hydration reaction, showed the highest strength. In contrast, sample 11 exhibited a slightly less effective hydration reaction and corresponding reduction in strength, whereas sample 9 demonstrated the least hydration and lowest strength.

3.6. XRD product analysis

Figure 12 shows the XRD test results, revealing similar hydration products in groups 1#, 9#, and 11# after aging for seven and 28 days. These products predominantly included calcite ($CaCO_3$), calcium hydroxide ($Ca(OH)_2$), ettringite (AFt), quartz (SiO_2), and hydrated calcium silicate (C-S-H). However, variations in the intensity and appearance of the diffraction peaks associated with the specific hydration products were evident across the groups.

A comparison of the XRD results for sample 1# at seven and 28 days showed slight changes in the diffraction peak patterns for each phase, indicating rapid hydration reactions within the initial seven days. By day 28, the $Ca(OH)_2$ peaks became more pronounced, likely due to the ongoing reactions of CaO. Moreover, the emergence of C-S-H diffraction peaks at 28 days signified the substantial formation of C-S-H in the later stages. In contrast, the intensities of the diffraction peaks for the various phases in sample 9# at seven and 28 days were generally lower than those of samples 1# and 11#, indicating less pronounced hydration products. This corresponds to the lower strength observed in concrete sample 9# during strength testing.

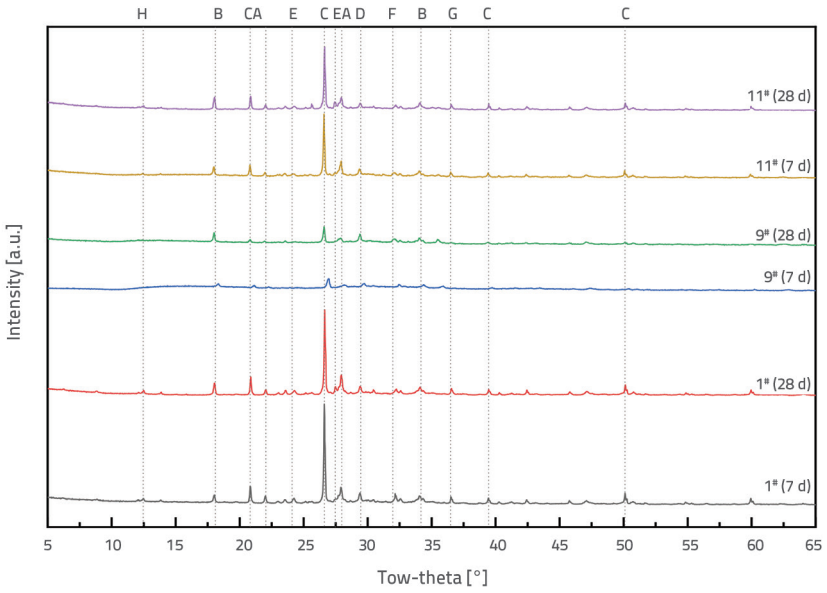

Figure 12. XRD pattern of hydration products of slag concrete (Samples 1#, 9#i 11#) (A: AFt; B: $Ca(OH)_2$; C: SiO_2; D: $CaCO_3$; E: C-S-H; F: CASH; G: $CaSiO_3$; H: $NaAlSiO_4$)

In sample 11#, the diffraction patterns of each physical phase exhibited a trend similar to that of sample 1# at both seven and 28 days. However, the intensities of these diffraction peaks were lower than those of sample 1#. The more pronounced diffraction peaks in sample 1 indicate a more thorough hydration reaction, which is consistent with the SEM results. These combined findings from the SEM and XRD analyses strongly support the observed trends in the mechanical properties of the slag concrete. Notably, distinct SiO_2 diffraction peaks were observed across all the specimens, primarily because of the presence of fly ash, with unhydrated fly ash contributing to the quartz phase. SEM images further illustrated that some unreacted fly ash acts as a filler material embedded within the internal microcracks and various pore in concrete, thereby densifying its internal structure.

The presence of $CaCO_3$ diffraction peaks in all the XRD results is attributed to the conversion of free calcium ions to $Ca(OH)_2$ in an alkaline environment during curing. Moreover, the alkaline curing process facilitates the formation of the $CaCO_3$ phase [35-37].

4. Economic and social benefits discussion

According to comprehensive price data for construction projects in Shihezi as of April 2024 [38], the cost of medium sand WAS $13.68 per cubic meter. Coal-fired slag from the Shihezi South Thermal Power Plant WAS priced at $3.53 per tonne, and the cost of simple crushing and screening of the coal-fired slag WAS $2.54 per tonne.

With an optimal coal-fired slag replacement ratio of 66.67 %, the amount of sand per cubic metre of concrete was 280 kg, and the amount of coal-fired slag was 560 kg. Compared with standard C30 commercial concrete priced at $47.24 per cubic meter, the cost of coal-fired slag concrete is reduced by approximately $1.71 per cubic meter, reflecting a cost reduction of approximately 3.62 %.

The use of coal-fired slag in construction is a sustainable practice that can significantly reduce the demand for river sand, thereby protecting aquatic ecosystems and stabilising riverbeds. Additionally, it utilises large quantities of slag, enhances its economic value, reduces soil and air pollution, and effectively turns waste into treasures.

5. Conclusion

This study focused on the production coal-fired slag concrete using power plant coal-fired slag, fly ash, cement, sand, and stone. The mechanical properties of the prepared concretes were evaluated using 16 sets of orthogonal tests on cubic samples. Based on these analyses, the key findings can be summarised as follows:

- An extreme variance analysis revealed that the water-cement ratio (A) had the most significant influence on the 28-day compressive and splitting tensile strengths of slag concrete, followed by the coal-fired slag replacement ratio (D), fly ash replacement ratio (B), and sand ratio (C). An increase in the water-cement and coal-fired slag replacement ratios led to a gradual decline in both the compressive and splitting tensile strengths of the concrete.
- XRD and SEM analyses revealed that the primary hydration products in the coal-fired slag concrete were AFt, $Ca(OH)_2$, SiO_2, $CaCO_3$, C-S-H, CASH, $CaSiO_3$, and $NaAlSiO_4$. As the curing progressed, these hydration products gradually filled the voids within the coal slag, leading to a denser microstructure and improved overall concrete strength. However, the incorporation of coal-slag particles introduced weaknesses in the concrete matrix. Under stress, cracks initially developed around the coal slag particles and propagated outwards, resulting in a reduction in the strength of the concrete with increased coal slag content.
- The optimal combination involved a water-cement ratio of 0.45, fly ash replacement ratio of 10 %, sand ratio of 45 %, and coal-fired slag replacement ratio of 66.67 %. This formulation produced concrete with excellent properties, achieving a slump of 187 mm, compressive strength of 42.18 MPa, and splitting tensile strength of 3.21 MPa. These results satisfy the stringent C30 strength requirements, making the concrete suitable for structural engineering applications. Additionally, this improvement reduced the cost of concrete per cubic meter by approximately 3.62 % compared with that of conventional concrete. This cost reduction not only

improves the economic viability of coal-fired slag, but also helps reduce the need for river sand mining, thereby supporting environmental conservation efforts.

- This study focused only on the compressive and splitting tensile strengths of slag concrete, which are insufficient for broader applications. Future research should include an in-depth analysis of the stress-strain behaviour and durability of slag concrete under loading conditions. The development of a constitutive model and energy dissipation theory for slag concrete can provide a foundation for advancing the seismic theory and its applications in reinforced slag concrete.

Acknowledgements

This study was funded by the Yili Normal University Research Project (2022YSYY002), Yili Prefecture Science and Technology Plan Project (YZ2022YD008), and Eighth Division Science and Technology Plan Project (2024GY03).

REFERENCES

[1] Institute CEPPE, China Energy Development Report 2023, People's Daily Press, Beijing, 2024

[2] Zhang, M., Lv, T., Deng, X., Dai, Y., Sajid, M.: Diffusion of China's coal-fired power generation technologies: historical evolution and development trends, Natural Hazards, 95 (2018), 1-2, 7-23, https://doi.org/10.1007/s11069-018-3524-4

[3] Jayaranjan, M.L.D., van Hullebusch, E.D., Annachhatre, A.P.: Reuse options for coal fired power plant bottom ash and fly ash, Reviews in Environmental Science and Bio/Technology, 13 (2014), 467-486, https://doi.org/10.1007/s11157-014-9336-4

[4] Mohammed, S.A., Koting, S., Katman, H.Y.B., Babalghaith, A.M., Abdul Patah, M.F., Ibrahim, M.R., Karim, M.R.: A review of the utilisation of coal bottom ash (CBA) in the Construction Industry, Sustainability, 13 (2021), https://doi.org/10.3390/su13148031

[5] Andreev, V., Bryukhan, F: Some Prospects for the use of ash and slag wastes of coal power plants for production of building materials, MATEC Web of Conferences, 86 (2016), https://doi.org/10.1051/matecconf/20168604004

[6] Ashish, D.K., Verma, S.K., Singh, J., Sharma, N.: Strength and durability characteristics of bricks made using coal bottom and coal fly ash, Advances in Concrete Construction, 6 (2018), 407422, https://doi.org/10.12989/acc.2018.6.4.407

[7] Siddique, R.: Utilization of coal combustion by-products in sustainable construction materials, Resources, Conservation and Recycling, 54 (2010), 1060-1066, https://doi.org/10.1016/j.resconrec.2010.06.011

[8] Skoko, B., Babić, D., Marović, G., Papić, S.: Environmental radiological risk assessment of a coal ash and slag disposal site with the use of the ERICA Tool, Journal of Environmental Radioactivity, 208-209 (2019), 106018, https://doi.org/10.1016/j.jenvrad.2019.106018

[9] Saha, D., Chatterjee, D., Chakravarty, S., Roychowdhury, T.: Investigation of environmental-concern trace elements in coal and their combustion residues from thermal power plants in Eastern India, Natural Resources Research, 28 (2019), 1505-1520, https://doi.org/10.1007/s11053-019-09451-2

[10] Stojanović, M., Radonjanin, V., Malešev, M., Milović, T., Furgan, S.: Compressive strength of cement stabilisations containing recycled and waste materials, GRAĐEVINAR, 73 (2021), 791-804, https://doi.org/10.14256/JCE.3161.2021

[11] Memiș, S., Ramroom, A.A.: Investigation of the use of waste mineral additives in ultra-high-performance concrete, Journal of the Croatian Association of Civil Engineers, 75 (2023) 06, 539-553, https://doi.org/10.14256/JCE.3305.2021

[12] Argiz, C., Menéndez, E., Moragues, A., Sanjuán, M.Á.: Recent advances in coal bottom ash use as a new common Portland cement constituent, Structural Engineering International, 24 (2014), 503-508, https://doi.org/10.2749/101686613X13768348400518

[13] Orna Carmona, M., González Paules, J., Sánchez Catalán, J..C, Fernández Pousa, L., Ade Beltrán, R., Quero Sanz, F.: Recycling power plant slag for use as aggregate in precast concrete components, Materiales de Construcción, 60 (2010), 99-113, https://doi.org/10.3989/mc.2010.52109

[14] Singh, M., Siddique, R.: Strength properties and micro-structural properties of concrete containing coal bottom ash as partial replacement of fine aggregate, Construction and Building Materials, 50 (2014), 246-256, https://doi.org/10.1016/j.conbuildmat.2013.09.026

[15] Verapathran, M., Palanisamy, M.: High performance concrete with steel slag aggregate, Gradevinar, 66 (2014) 7, 605-612, 10.14256/JCE.1052.2014

[16] Horiguchi, I., Shirai, A., Watanabe, M., Sugihara, S.: Fundamental study on concrete with coal gasification slag, Cement Science and Concrete Technology, 66 (2012), 615-621, https://doi.org/10.14250/cement.66.615

[17] Rui, Z., Tao, Z.: Experimental research on compressive strength of waste incineration bottom ash concrete, Bulletin of the Chinese Ceramic Society, 29 (2010) 02, 352-356 + 360, 10.16552/j.cnki.issn1001-1625.2010.02.044

[18] Geçkil, T., Tanyıldızı, M.M., İnce, C.B.: Benefit–cost relationship of using concrete with blast furnace slag as road pavement, Journal of the Croatian Association of Civil Engineers, 75 (2023), 23-37, https://doi.org/10.14256/JCE.3570.2022

[19] Murko, V., Khyamyalyainen, V., Baranova, M.: Use of ash-and-slag wastes after burning of fine-dispersed coal-washing wastes, E3S Web of Conferences, 41 (2018), 10.1051/e3sconf/20184101042

[20] Guo, Z., Liu, W., Wang, C., He, C., Zhang, F.: Fractal characteristics of mesostructure and optimisation of axial compression constitutive model of coal-fired slag concrete, Materials Today Communications, 28 (2021), 102686, https://doi.org/10.1016/j.mtcomm.2021.102686

[21] Poudel, S., Menda, S., Useldinger-Hoefs, J., Guteta, L.E., Dockter, B., Gedafa, D.S.: The use of ground coal bottom ash/slag as a cement replacement for sustainable concrete infrastructure, Materials, 17 (2024), 2316, 10.3390/ma17102316

[22] Jianpeng, Z., Gang, L., Yuwei, M., Hua, T., Haifeng, X., Fangfang, Y., Pengfei, S., Yangmei, Z.: Experimental study on the performance of the self-compacting slag concrete, New Building Materials, 44 (2017) 1010-0043-03, 43-45 + 76, 1001-1702X

[23] Liu, W., Niu, S.: Energy evolution properties and strength failure criterion of coal-fired slag concrete based on energy dissipation, Case Studies in Construction Materials, 17 (2022), e01369, https://doi.org/10.1016/j.cscm.2022.e01369

[24] Weizhen, L., Zhongping, G., Weisheng, H., Shuhong, H., Wenbo, H.: Experimental study on the ratio and strength characteristics of coal-fired slag concrete, Mining Research and Development, 40 (2020) 05, 56-59, 10.13827/j.cnki.kyyk.2020.05.011

[25] Liu, W., Guo, Z., Niu, S., Hou, J., Zhang, F., He, C.: Mechanical properties and damage evolution behaviour of coal–fired slag concrete under uniaxial compression based on acoustic emission monitoring technology, Journal of Materials Research and Technology, 9 (2020), 9537-9549, https://doi.org/10.1016/j.jmrt.2020.06.071

[26] Common Portland Cement, 2007, GB175-2007

[27] Specification for mix proportion design of ordinary concrete, 2011, JGJ 55-2011

[28] Standard for test methods for properties of ordinary concrete mixes, 2016, GB/T 50080-2016

[29] Standard of test methods for physical and mechanical properties of concrete, 2019, GB/T 50081-2019

[30] Singh, M., Siddique, R.: Effect of coal bottom ash as partial replacement of sand on workability and strength properties of concrete, Journal of Cleaner Production, 112 (2016), 620-630, https://doi.org/10.1016/j.jclepro.2015.08.001

[31] Juntao, H., Xiangdong, S.: Experimental study on early mechanical properties of natural lightweight aggregate concrete with external mixing fly ash, Bulletin of the Chinese Ceramic Society, 31 (2012) 04, 847-851, 10.16552/j.cnki.issn1001-1625.2012.04.011

[32] Kou, S.C., Poon, C.S., Chan, D.: Influence of fly ash as cement replacement on the properties of recycled aggregate concrete, Journal of Materials in Civil Engineering, 19 (2007), 709-717, 10.1061/(ASCE)0899-1561(2007)19:9(709)

[33] General code for concrete structures, 2021, GB 55008-2021

[34] Licheng, W., Lei, Z.: Research progress on concrete internal curing technology journal of building materials, 23 (2020) 06, 1471-1478, 10.3969/j.issn.10079629.2020.06028

[35] Ma, X., He, T., Xu, Y., Yang, R., Sun, Y.: Hydration reaction and compressive strength of small amount of silica fume on cement-fly ash matrix, Case Studies in Construction Materials, 16 (2022), e00989, https://doi.org/10.1016/j.cscm.2022.e00989

[36] Chanda, S.S., Patel, S.K., Nayak, A.N., Mohanty, C.R.: Performance evaluation on bond, durability, micro-structure, cost effectiveness and environmental impacts of fly ash cenosphere based structural lightweight concrete, Construction and Building Materials, 397 (2023), 132429, https://doi.org/10.1016/j.conbuildmat.2023.132429

[37] Raju, S., Dharmar, B.: Durability characteristics of copper slag concrete with fly ash, Gradevinar, 69 11 (2017), 1031-1040, 10.14256/jce.1229.2015

[38] Compilation Explanation of Comprehensive Price Information for Construction Projects in Shihezi Area in April 2024 http://www.shz.gov.cn/govxxgk/014/2024-05-17/c3f7f9d9-1c3e-431a-8842-2c31f4d284c3.html, 17.05.2024